LETTERS
PUBLISHED ONLINE: 31 JULY 2011 | DOI: 10.1038/NMAT3066
nature materials

A lithium superionic conductor

Noriaki Kamaya[1], Kenji Homma[1], Yuichiro Yamakawa[1], Masaaki Hirayama[1], Ryoji Kanno[1]*, Masao Yonemura[2], Takashi Kamiyama[2], Yuki Kato[3], Shigenori Hama[3], Koji Kawamoto[3] and Akio Mitsui[4]

Batteries are a key technology in modern society[1,2]. They are used to power electric and hybrid electric vehicles and to store wind and solar energy in smart grids. Electrochemical devices with high energy and power densities can currently be powered only by batteries with organic liquid electrolytes. However, such batteries require relatively stringent safety precautions, making large-scale systems very complicated and expensive. The application of solid electrolytes is currently limited because they attain practically useful conductivities (10^{-2} S cm^{-1}) only at 50–80 °C, which is one order of magnitude lower than those of organic liquid electrolytes[3–8]. Here, we report a lithium superionic conductor, $Li_{10}GeP_2S_{12}$ that has a new three-dimensional framework structure. It exhibits an extremely high lithium ionic conductivity of 12 mS cm^{-1} at room temperature. This represents the highest conductivity achieved in a solid electrolyte, exceeding even those of liquid organic electrolytes. This new solid-state battery electrolyte has many advantages in terms of device fabrication (facile shaping, patterning and integration), stability (non-volatile), safety (non-explosive) and excellent electrochemical properties (high conductivity and wide potential window)[9–11].

The great demand for batteries with high power and energy densities promotes the need for advanced lithium-ion and lithium–air battery technologies[1,2]. Solid electrolytes promise the potential to replace organic liquid electrolytes and thereby improve the safety of next-generation high-energy batteries. Although the advantages of non-flammable solid electrolytes are widely acknowledged, their low ionic conductivities and low chemical and electrochemical stabilities prevent them being used in practical applications.

In an effort to overcome these problems, there has been an ongoing search over the past few decades for new materials for solid electrolytes. This search has considered crystalline, glassy, polymer and composite systems. Despite these efforts, lithium nitride (Li_3N), which was discovered in the 1970s (ref. 12), still has the highest ionic conductivity (6×10^{-3} S cm^{-1} at room temperature) of potential solid electrolytes[13]. Unfortunately, its low electrochemical decomposition potential prevents it being used in practical applications. Other systems currently being investigated as battery electrolytes are crystalline materials (such as oxide perovskite, $La_{0.5}Li_{0.5}TiO_3$ (ref. 3) and thio-LISICON, $Li_{3.25}Ge_{0.25}P_{0.75}S_4$ (ref. 4)), glass ceramics ($Li_7P_3S_{11}$; refs 5,6) and glassy materials (Li_2S–SiS_2–Li_3PO_4; refs 7,8); all these materials exhibit ionic conductivities of the order of 10^{-3} S cm^{-1}, which is lower than that of lithium nitride. Polymer electrolytes are commonly complexes of a lithium salt and high-molecular-weight polymers, such as polyethylene oxide, and they have very low conductivities at room temperature ($\sim 10^{-5}$ S cm^{-1}; refs 14, 15). None of these materials have conductivities comparable to those of organic liquid electrolytes and currently used lithium-ion systems (generally of the order of 10^{-2} S cm^{-1} at room temperature[16]).

Lithium superionic conductors, which can be used as solid electrolytes, exhibit a high ionic diffusion in the mobile ion sublattice at temperatures well below their melting points. It is very important to understand the mechanism for fast ionic transport in solids (although it is still a relatively unusual phenomenon). It is also a challenging problem to synthesize new lithium superionic conductors. The new $Li_{10}GeP_2S_{12}$ with a one-dimensional conduction pathway exhibits an extremely high bulk conductivity of over 10^{-2} S cm^{-1} at room temperature (27 °C). An all-solid-state battery with the structure $LiCoO_2$/$Li_{10}GeP_2S_{12}$/In exhibits an excellent battery performance.

$Li_{10}GeP_2S_{12}$ was synthesized by reacting stoichiometric quantities of Li_2S, GeS_2 and P_2S_5 at 550 °C in an evacuated quartz tube. The X-ray diffraction (XRD) pattern of the reaction product indicates a new phase with structure that differs from those of previously reported superionic conductors such as thio-LISICON (ref. 4) and Li_7PS_6 (ref. 5). The P/Ge ratio was determined by inductively coupled plasma (ICP) spectroscopy and found to be 0.662:0.338; this value is consistent with the stoichiometric ratio of P/Ge = 2.

The composition and structure of $Li_{10}GeP_2S_{12}$ was determined by synchrotron XRD and neutron diffraction measurements. Peak indexing of the synchrotron XRD pattern revealed that the new phase has a tetragonal unit cell with cell parameters of $a = 8.71771(5)$ Å and $c = 12.63452(10)$ Å and with the extinction rule $hk0 : h + k = 2n$, $hhl : l = 2n$, $00l : l = 2n$ and $h00 : h = 2n$, which is characteristic of the space group $P4_2/nmc$ (137). An *ab initio* structure analysis determined the arrangement of PS_4 and GeS_4 tetrahedra in the unit cell. Synchrotron X-ray Rietveld refinements obtained using the structural model determined by the *ab initio* method revealed low agreement factors. On the basis of the structural model obtained by synchrotron XRD data analysis, the positions of lithium ions and the lithium content were determined by neutron Rietveld analysis. Profile fitting using the neutron diffraction data also provided low agreement factors. Supplementary Fig. S1 shows a neutron Rietveld refinement pattern. Supplementary Table S1 summarizes the *R* factors, lattice parameters and final structure parameters determined by the refinement process. The unit cell has two tetrahedral sites: 4*d* and

[1]Department of Electronic Chemistry, Interdisciplinary Graduate School of Science and Engineering, Tokyo Institute of Technology, 4259 Nagatsuta, Midori, Yokohama 226-8502, Japan, [2]Neutron Science Laboratory (KENS), Institute of Materials Structure Science, High Energy Accelerator Research Organization (KEK), 1-1 Oho, Tsukuba, Ibaraki 305-0801, Japan, [3]Toyota Motor Corporation, Battery Research Division, Higashifuji Technical Center, 1200 Mishuku, Susono, Shizuoka 410-1193, Japan, [4]Toyota Motor Corporation, Material Engineering Management Division, Material Analysis Department, 1 Toyota-cho, Toyota, Aichi 471-8572, Japan. *e-mail: kanno@echem.titech.ac.jp.

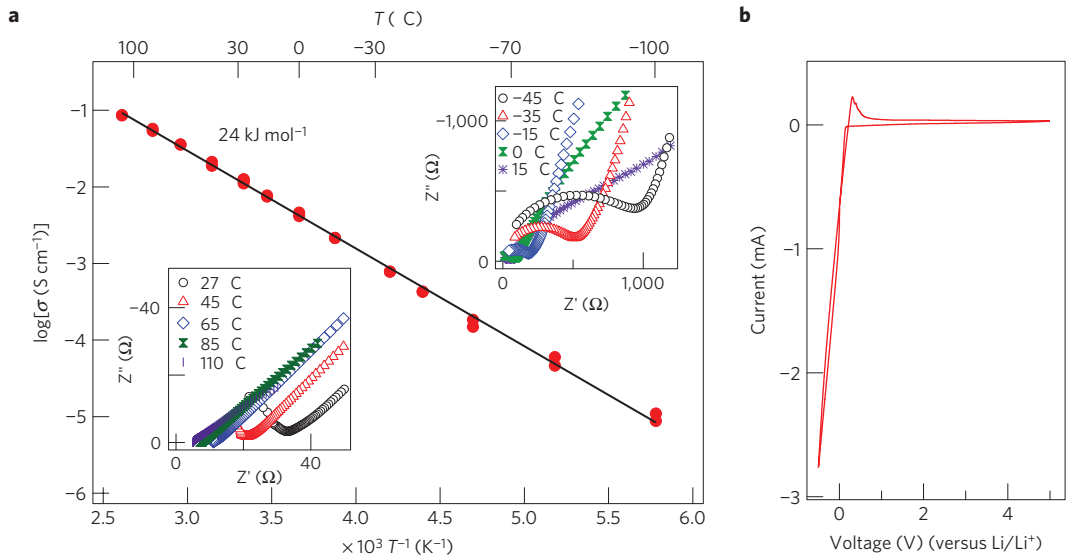

Figure 1 | Lithium-ion conductivity of $Li_{10}GeP_2S_{12}$. a, Impedance plots of the conductivity data from low to high temperatures and Arrhenius conductivity plots of $Li_{10}GeP_2S_{12}$. The plotted conductivity represents the sum of the grain boundary and bulk conductivities. $Li_{10}GeP_2S_{12}$ exhibits an extremely high ionic conductivity even at room temperature. **b**, Current–voltage curve of Li/$Li_{10}GeP_2S_{12}$/Au cell. The decomposition potential of the new $Li_{10}GeP_2S_{12}$ phase exceeds 5 V.

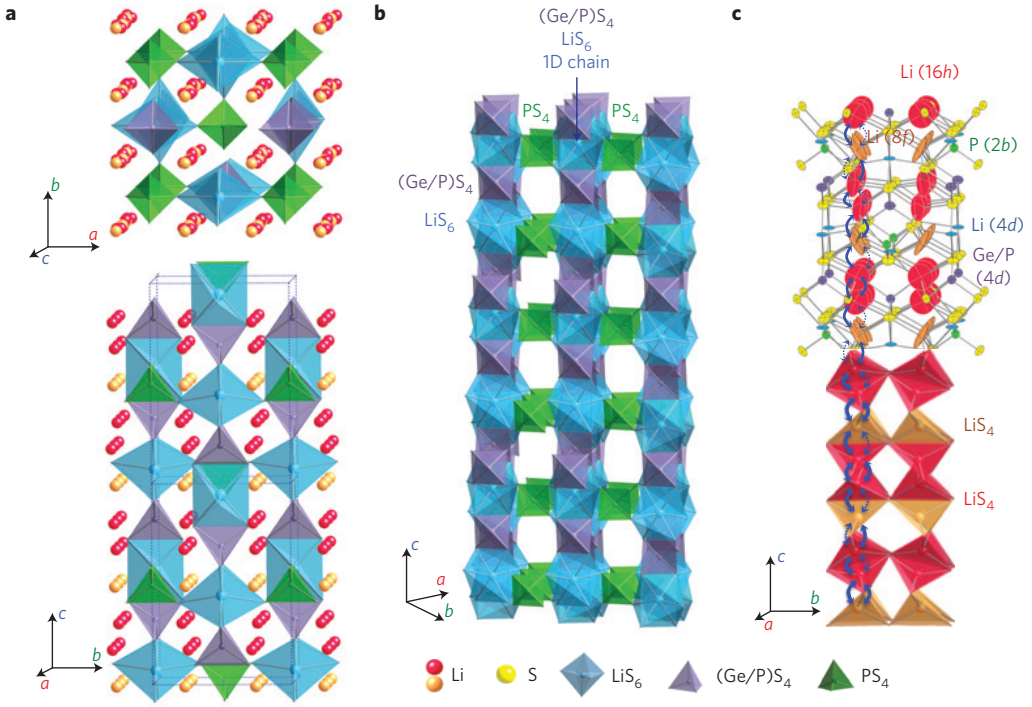

Figure 2 | Crystal structure of $Li_{10}GeP_2S_{12}$. a, The framework structure and lithium ions that participate in ionic conduction. **b**, Framework structure of $Li_{10}GeP_2S_{12}$. One-dimensional (1D) chains formed by LiS_6 octahedra and $(Ge_{0.5}P_{0.5})S_4$ tetrahedra, which are connected by a common edge. These chains are connected by a common corner with PS_4 tetrahedra. **c**, Conduction pathways of lithium ions. Zigzag conduction pathways along the *c* axis are indicated. Lithium ions in the LiS_4 tetrahedra (16*h* site) and LiS_4 tetrahedra (8*f* site) participate in ionic conduction. Thermal ellipsoids are drawn with a 30% probability. The anisotropic character of the thermal vibration of lithium ions in three tetrahedral sites gives rise to 1D conduction pathways.

2*b* sites. The 4*d* tetrahedral site is occupied by Ge and P ions with occupancy parameters of 0.515(5) and 0.485(5), respectively. The 2*b* tetrahedral site is occupied only by P with an occupancy parameter of 1.00(15). The Ge/P ratio is then 4.06:1.94, which is very close to the stoichiometric ratio of 2:1 and is consistent with the composition determined by ICP analysis. There are three lithium sites in the unit cell: 16*h*, 4*d* and 8*f* sites, with occupancy parameters of 0.691(5), 1.000(8) and 0.643(5), respectively. The number of lithium atoms in the unit cell is then calculated to be 20.200. On the basis of the ICP and neutron diffraction analyses, the composition of the new phase was determined to be $Li_{10}GeP_2S_{12}$.

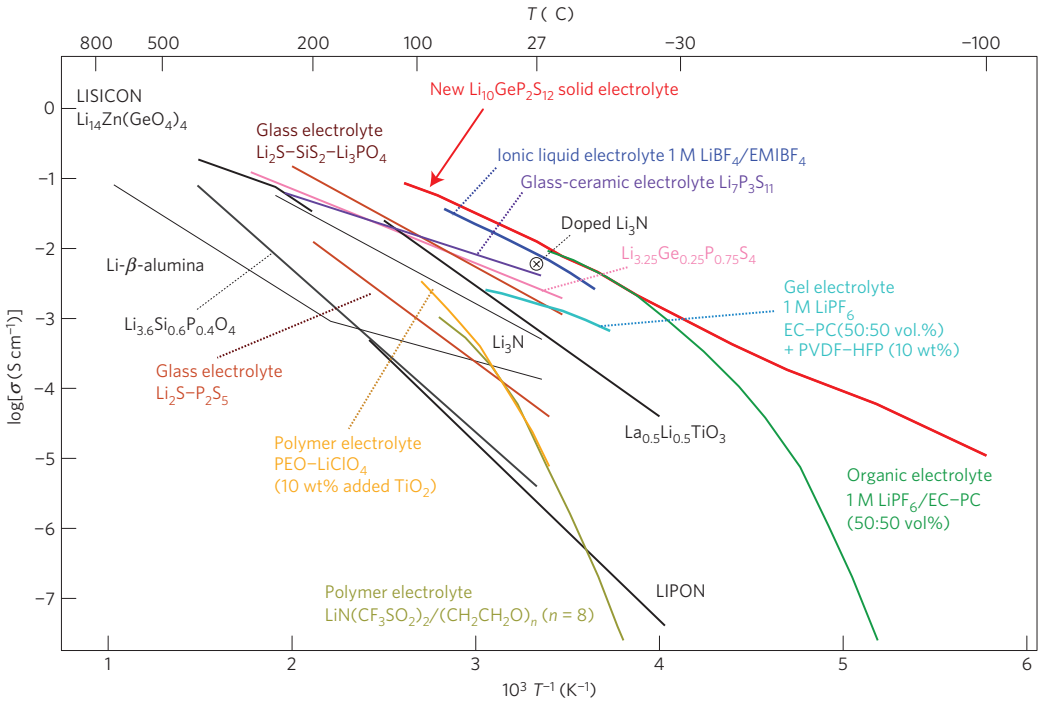

Figure 3 | Thermal evolution of ionic conductivity of the new $Li_{10}GeP_2S_{12}$ phase, together with those of other lithium solid electrolytes, organic liquid electrolytes, polymer electrolytes, ionic liquids and gel electrolytes[3–8,13–16,20,22]. The new $Li_{10}GeP_2S_{12}$ exhibits the highest lithium ionic conductivity (12 m S cm^{-1} at 27 °C) of the solid lithium conducting membranes of inorganic, polymer or composite systems. Because organic electrolytes usually have transport numbers below 0.5, inorganic lithium electrolytes have extremely high conductivities.

Figure 1 shows the conductivity measurement results for the $Li_{10}GeP_2S_{12}$ produced in the present study. The conductivity was calculated from the impedance plots shown in Fig. 1a, which are characteristic of pure ionic conductors; they consist of a semicircle and a spike, which respectively correspond to contributions from the bulk/grain boundary and the electrode. The conductivity was obtained from the sum of the grain boundary and bulk resistances. The conductivity of 12 mS cm^{-1} at 27 °C is extremely high. To the best of our knowledge, this is the highest ionic conductivity reported for a lithium superionic conductor. It is comparable to or higher than the conductivities of practical organic liquid electrolytes used in lithium-ion batteries. The activation energies for ionic conduction were calculated to be 24 kJ mol^{-1} for the temperature range of −110 to 110 °C, which are typical activation energies for superionic conductors.

We evaluated the electrochemical stability from the cyclic voltammogram of a Li/$Li_{10}GeP_2S_{12}$/Au cell with a lithium reference electrode at a scan rate of 1 mV s^{-1} and a scan range of −0.5 to 5 V (Fig. 1b). Cathodic and anodic currents respectively corresponding to lithium deposition ($Li^+ + e^- \rightarrow Li$) and dissolution ($Li \rightarrow Li^+ + e^-$) were observed near 0 V. No significant currents due to electrolyte decomposition were detected in the scanned voltage range. Crystalline materials with high ionic conductivities such as Li_3N and $Li_{1/3-x}Li_{3x}NbO_3$ have low electrochemical stabilities; for example, Li_3N (ref. 17) has a decomposition potential of 0.44 V and $La_{1/3-x}Li_{3x}NbO_3$ perovskite[18] has a reduction potential of 1.7 V. The present $Li_{10}GeP_2S_{12}$ has both a high ionic conductivity and a high decomposition potential. The electronic conductivity was measured by the Hebb–Wagner polarization method[19] using a (−)Li/$Li_{10}GeP_2S_{12}$/Au(+) cell at 25 °C. The total electronic conductivity (electron + hole) at the irreversible Au–$Li_{10}GeP_2S_{12}$ interface of the asymmetric cell was calculated to be 5.70×10^{-9} S cm^{-1} by linear fitting between 2.8 and 3.5 V.

The new superionic conductor $Li_{10}GeP_2S_{12}$ has a three-dimensional framework structure consisting of $(Ge_{0.5}P_{0.5})S_4$ tetrahedra, PS_4 tetrahedra, LiS_4 tetrahedra and LiS_6 octahedra. This framework structure has a one-dimensional (1D) lithium conduction pathway along the c axis. Figure 2 shows the crystal structure of $Li_{10}GeP_2S_{12}$. The framework is composed of $(Ge_{0.5}P_{0.5})S_4$ tetrahedra and LiS_6 octahedra, which share a common edge and form a 1D chain along the c axis. These 1D chains are connected to one another through PS_4 tetrahedra, which are connected to LiS_6 octahedra by a common corner (see Fig. 2b). The 1D conduction pathway is formed by LiS_4 tetrahedra in the 16h and 8f sites, which share a common edge and form a 1D tetrahedron chain. These chains are connected by common corners of the LiS_4 tetrahedra (Fig. 2c). Neutron diffraction analysis indicates that the thermal vibration of lithium at the 16h and 8f sites is highly anisotropic (Fig. 2c). The anisotropic thermal displacements indicate that lithium is displaced from the 16h and 8f sites toward interstitial positions between two 16h sites and between 16h and 8f sites. This clearly indicates the existence of 1D conduction pathways along the c axis. The occupancy parameters of 16h and 8f sites (determined respectively to be 0.691(5) and 0.643(5)) indicate partially occupied sites and show the average distribution of lithium ions along the conduction pathway, which is a characteristic of superionic conductors.

Figure 3 shows the thermal evolution of the ionic conductivity of the new $Li_{10}GeP_2S_{12}$ phase together with those of other electrolytes used in practical batteries. For example, the organic liquid electrolyte ethylene carbonate (EC)–propylene carbonate (PC) (50:50 vol.%) containing 1 M $LiPF_6$ (ref. 16) has a conductivity of 10^{-2} S cm^{-1} at room temperature. A gel electrolyte, such as 1 M $LiPF_6$/EC–PC (50:50 vol.%) + polyvinylidene difluoride–hexafluoropropylene (10 wt%; ref. 20), which is currently used in practical lithium-ion batteries to enhance their safety, has a slightly lower ionic conductivity than liquid electrolytes. Even at low temperatures, $Li_{10}GeP_2S_{12}$ has a very high conductivity (1 mS cm^{-1} at −30 °C and 0.4 mS cm^{-1} at −45 °C), which will enable practical batteries to operate at low temperatures; this is one advantage of

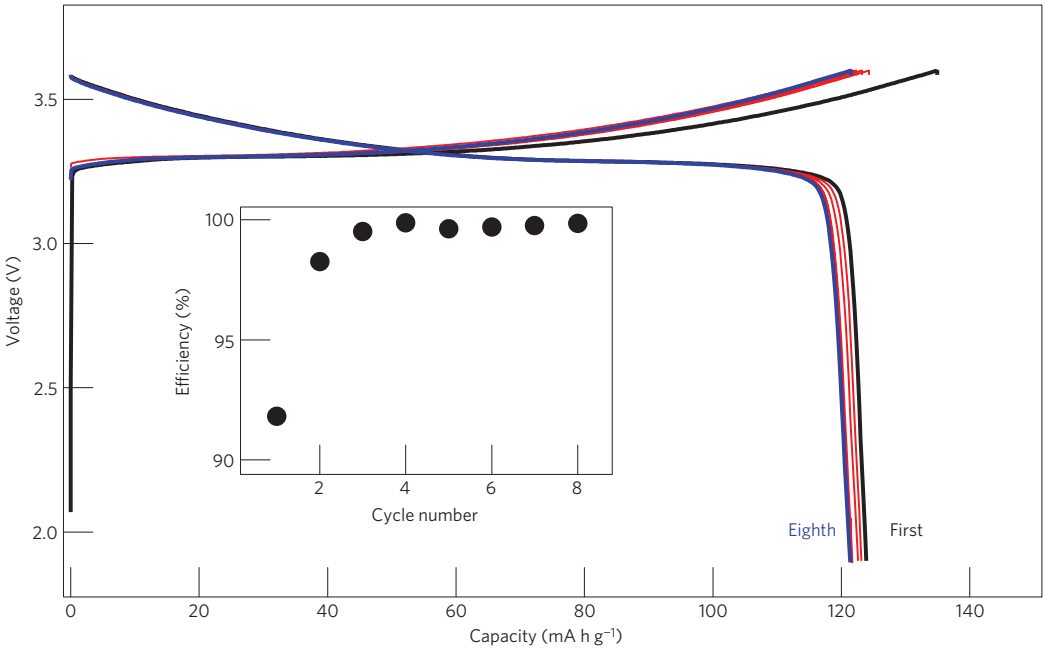

Figure 4 | Charge–discharge curves of an all-solid-state battery consisting of a $LiCoO_2$ cathode, a $Li_{10}GeP_2S_{12}$ electrolyte and an In metal anode. The current density is 14 mA g^{-1}. The battery has a discharge capacity of over 120 mA h g^{-1} and an excellent discharge efficiency of about 100% after the second cycle, demonstrating that $Li_{10}GeP_2S_{12}$ is suitable as an electrolyte for all-solid-state batteries.

solid electrolytes over organic electrolytes. Many materials have been proposed for overcoming the safety problems associated with high-energy-density batteries. Figure 3 also shows the ionic conductivities of an inorganic solid electrolyte (Li_2S–P_2S_5), an ionic liquid (1 M $LiBF_4$/1-ethyl-3-methylimidazolium tetrafluoroborate[21]) and a polymer electrolyte, LiN $(CF_3SO_2)_2/(CH_2CH_2O)_n$ ($n = 8$; ref. 14). These electrolytes have conductivities that are several orders of magnitude lower than those of organic liquid electrolytes. The present $Li_{10}GeP_2S_{12}$ is the first electrolyte that has an ionic conductivity that is comparable to or even higher than those of liquid organic systems and much higher chemical and thermal stabilities.

The new electrolyte $Li_{10}GeP_2S_{12}$ was examined as a solid electrolyte for practical lithium batteries. Figure 4 shows charge–discharge curves of an all-solid-state battery, which consisted of a $LiCoO_2$ cathode, a $Li_{10}GeP_2S_{12}$ electrolyte and an In metal anode, at a current density of 14 mA g^{-1}. The battery exhibits a discharge capacity of over 120 mA h g^{-1} and an excellent discharge efficiency of about 100% after the second cycle, demonstrating that $Li_{10}GeP_2S_{12}$ is applicable as a practical electrolyte for all-solid-state batteries.

In conclusion, the results presented here reveal that the new $Li_{10}GeP_2S_{12}$ phase has an extremely high ionic conductivity that is higher than the lithium-ion conductivity of any other lithium superionic conductor. Room-temperature conductivities of 12 mS cm^{-1} are comparable to or higher than those of organic liquid electrolytes currently used in practical lithium-ion systems. The discovery of a new solid electrolyte will result in a wide range of fundamental studies on ionic mobility in the bulk material and this will lead to the development of next-generation batteries. Our new lithium solid electrolyte is promising for applications requiring batteries with high powers and energy densities, and for pure electric and hybrid electric vehicles and other electrochemical devices that require high safety, stability and reliability.

Methods

Synthesis. The starting materials were Li_2S (Idemitsu Kosan, >99.9% purity), P_2S_5 (Aldrich, >99% purity) and GeS_2 (Aldrich, >99% purity). These were weighed, mixed in the molar ratio of $Li_2S/P_2S_5/GeS_2$ to 5/1/1 in an Ar-filled glove box, placed into a stainless-steel pot and mixed for 30 min using a vibrating mill (CMT, Tl-100). The specimens were then pressed into pellets, sealed in a quartz tube at 30 Pa and heated at a reaction temperature of 550 °C for 8 h in a furnace. After reacting, the tube was slowly cooled to room temperature. XRD (Rigaku, SmartLab and Ultima) analysis was used to confirm the formation of a single phase. The P/Ge ratio was determined by ICP spectroscopy (iCAP, Thermo Scientific).

Crystal structure analysis. In the structural analysis process, the framework structure consisting of germanium and phosphorus sulphide polyhedra and the positions of lithium atoms were determined on the basis of synchrotron and neutron diffraction data. XRD data were obtained using a high-flux synchrotron X-ray source at the BL02B2 beamline at SPring-8. A Debye–Scherrer diffraction camera was used for the measurements at −173 °C. The specimen was sealed in a quartz capillary (about 0.3 mm diameter) in a vacuum for the XRD measurements. Diffraction data were collected in 0.01° steps from 3.0° to 70.0° in 2θ. The incident-beam wavelength was calibrated using NIST SRM Ceria 640b CeO_2 and fixed at 0.59960 Å. The unit-cell parameters of the new phase were indexed using 20 reflections in the XRD data and the autoindexing program DICVOL (ref. 22). The validity of the space group was determined by subsequent structural analysis (that is, structure modelling by the *ab initio* method and structural refinement by the Rietveld method). The crystal structure was solved directly by the *ab initio* method by global optimization of a structural model in direct space using the program FOX (ref. 23). PS_4 and GeS_4 tetrahedra (with expected Ge–S and P–S bond lengths of respectively 2.1 and 2.0 Å in the asymmetric unit) were used as the building blocks in the initial configuration of the *ab initio* method. The program randomly moves and rotates PS_4 and GeS_4 tetrahedra in real space, calculates the corresponding powder diffraction pattern and searches for the best structure that reproduces the observed diffraction pattern. The initial structure was then refined by the Rietveld method using the RIETAN-FP programme[24]. The positions of some of the lithium ions were investigated by plotting a Fourier map using the synchrotron diffraction data. Neutron Rietveld analysis was carried out to accurately determine the positions and occupancy parameters of the lithium sites. The neutron diffraction data were obtained using a high-resolution neutron powder diffractometer, Super HRPD (BL08), at the neutron radiation facility centre J-PARC in Tokai, Japan. The specimen was sealed in a vanadium cell (about 6 mm diameter) using an indium ring. The crystal structure was refined by the Rietveld method using the Z-Rietveld programme[25]. The positions of lithium ions were investigated by plotting a Fourier map and refining the positions and occupancy parameters. In the final refinement cycle, anisotropic thermal parameters were refined for all the atomic positions. Synchrotron X-ray and neutron Rietveld analysis clarified the positions of all the lithium atoms in $Li_{10}GeP_2S_{12}$.

Ionic and electronic conductivities. The $Li_{10}GeP_2S_{12}$ powder was pressed into a pellet (diameter 10 mm; thickness 3–4 mm) in an Ar atmosphere. It was then coated with Au to form an electrode and heated to 500 °C in a vacuum before measuring

the ionic conductivity. The a.c. impedance of the Au/$Li_{10}GeP_2S_{12}$/Au cell was measured between −110 and 110 °C in an Ar atmosphere; this was repeated two or three times by applying 100–500 mV in a frequency range 10^6–10^{-1} Hz using a frequency response analyser (Solartron, 1260). The cyclic voltammogram of the Li/$Li_{10}GeP_2S_{12}$/Au cell was measured using a lithium reference with a scan rate of 1 mV s^{-1} between −0.5 and 5.0 V at 25 °C. The electrical conductivity was investigated by the Hebb–Wagner polarization method[19].

Charge–discharge measurements. The cathode consisted of $LiNbO_3$-coated $LiCoO_2$ and $Li_{10}GeP_2S_{12}$. The $LiNbO_3$ layer was coated on a commercial $LiCoO_2$ powder (Toda Kogyo) using a fluidized bed granulator (MP-01, Powrex; ref. 26). The $LiNbO_3$-coated $LiCoO_2$ and $Li_{10}GeP_2S_{12}$ were weighed in the ratio of 70:30 (wt%) and mixed using a vortex mixer for 5 min. The $LiCoO_2$/$Li_{10}GeP_2S_{12}$/In cell was assembled using an indium plate (Nilaco; thickness 0.1 mm; diameter 10 mm) as an anode. The electrochemical properties of the cells were determined using a TOSCAT-3100 (Toyo System). A cycling test was carried out between 1.9 and 3.6 V at an applied current of 14 mA g^{-1} at 25 °C.

Received 26 November 2010; accepted 9 June 2011; published online 31 July 2011

References

1. Tarascon, J. M. & Armand, M. Issues and challenges facing rechargeable lithium batteries. *Nature* **414,** 359–367 (2001).
2. Armand, M. & Tarascon, J. M. Building better batteries. *Nature* **451,** 652–657 (2008).
3. Inaguma, Y. *et al.* High ionic-conductivity in lithium lanthanum titanate. *Solid State Commun.* **86,** 689–693 (1993).
4. Kanno, R. & Maruyama, M. Lithium ionic conductor thio-LISICON—the Li_2S–GeS_2–P_2S_5 system. *J. Electrochem. Soc.* **148,** A742–A746 (2001).
5. Mizuno, F., Hayashi, A., Tadanaga, K. & Tatsumisago, M. New, highly ion-conductive crystals precipitated from Li_2S–P_2S_5 glasses. *Adv. Mater.* **17,** 918–921 (2005).
6. Hayashi, A., Minami, K., Mizuno, F. & Tatsumisago, M. Formation of Li^+ superionic crystals from the Li_2S–P_2S_5 melt-quenched glasses. *J. Mater. Sci.* **43,** 1885–1889 (2008).
7. Kondo, S., Takada, K. & Yamamura, Y. New lithium ion conductors based on Li_2S–SiS_2 system. *Solid State Ion.* **53,** 1183–1186 (1992).
8. Takada, K., Aotani, N. & Kondo, S. Electrochemical behaviors of Li^+ ion conductor, Li_3PO_4–Li_2S–SiS_2. *J. Power Sources* **43,** 135–141 (1993).
9. Inada, T. *et al.* All solid-state sheet battery using lithium inorganic solid electrolyte, thio-LISICON. *J. Power Sources* **194,** 1085–1088 (2009).
10. Kobayashi, T. *et al.* All solid-state battery with sulfur electrode and thio-LISICON electrolyte. *J. Power Sources* **182,** 621–625 (2008).
11. Kobayashi, T., Yamada, A. & Kanno, R. Interfacial reactions at electrode/electrolyte boundary in all solid-state lithium battery using inorganic solid electrolyte, thio-LISICON. *Electrochim. Acta* **53,** 5045–5050 (2008).
12. Alpen, U. V., Rabenau, A. & Talat, G. H. Ionic-conductivity in Li_3N single-crystals. *Appl. Phys. Lett.* **30,** 621–623 (1977).
13. Lapp, T., Skaarup, S. & Hooper, A. Ionic-conductivity of pure and doped Li_3N. *Solid State Ion.* **11,** 97–103 (1983).
14. Edman, L., Ferry, A. & Doeff, M. M. Slow recrystallization in the polymer electrolyte system poly(ethylene oxide)(n)-LiN(CF_3SO_2)(2). *J. Mater. Res.* **15,** 1950–1954 (2000).
15. Croce, F., Appetecchi, G. B., Persi, L. & Scrosati, B. Nanocomposite polymer electrolytes for lithium batteries. *Nature* **394,** 456–458 (1998).
16. Stallworth, P. E. *et al.* NMR, DSC and high pressure electrical conductivity studies of liquid and hybrid electrolytes. *J. Power Sources* **81,** 739–747 (1999).
17. Rabenau, A. Lithium nitride and related materials—case-study of the use of modern solid-state research techniques. *Solid State Ion.* **6,** 277–293 (1982).
18. Garcia-Martin, S., Rojo, J. M., Tsukamoto, H., Moran, E. & Alario-Franco, M. A. Lithium-ion conductivity in the novel $La_{1/3-x}Li_{3x}NbO_3$ solid solution with perovskite-related structure. *Solid State Ion.* **116,** 11–18 (1999).
19. Neudecker, B. J. & Weppner, W. Li_9SiAlO_8: A lithium ion electrolyte for voltages above 5.4 V. *J. Electrochem. Soc.* **143,** 2198–2203 (1996).
20. Song, J. Y., Wang, Y. Y. & Wan, C. C. Conductivity study of porous plasticized polymer electrolytes based on poly(vinylidene fluoride)—A comparison with polypropylene separators. *J. Electrochem. Soc.* **147,** 3219–3225 (2000).
21. Saruwatari, H., Kuboki, T., Kishi, T., Mikoshiba, S. & Takami, N. Imidazolium ionic liquids containing LiBOB electrolyte for lithium battery. *J. Power Sources* **195,** 1495–1499 (2010).
22. Boultif, A. & Louer, D. Indexing of powder diffraction patterns for low-symmetry lattice by the successive dichotomy method. *J. Appl. Crystallogr.* **24,** 987–993 (1991).
23. Favre-Nicolin, V. & Cerny, R. FOX, 'free objects for crystallography': A modular approach to *ab initio* structure determination from powder diffraction. *J. Appl. Crystallogr.* **35,** 734–743 (2002).
24. Izumi, F. & Momma, K. Three-dimensional visualization in powder diffraction. *Solid State Phenom.* **130,** 15–20 (2007).
25. Oishi, R. *et al.* Rietveld analysis software for J-PARC. *Nucl. Instrum. Methods Phys. Res.* **600,** 94–96 (2009).
26. Ohta, N. *et al.* $LiNbO_3$-coated $LiCoO_2$ as cathode material for all solid-state lithium secondary batteries. *Electrochem. Commun.* **9,** 1486–1490 (2007).

Acknowledgements

This work was partially supported by a Grant-in-Aid for Scientific Research (A) from the Japan Society for the Promotion of Science. The synchrotron and neutron radiation experiments were carried out as projects approved by the Japan Synchrotron Radiation Research Institute (JASRI) (proposal No 2010A1584) and the Japan Proton Accelerator Research Complex (J-PARC) and Institute of Materials Structure Science (proposal No 2009B0039 and No. 2010A0060), respectively.

Author contributions

N.K. and Y.Y. conceived the synthesis experiments and the electrochemical characterization. K.H., M.Y. and T.K. carried out the structural analysis. M.H. and R.K. analysed the data and wrote the manuscript. Y.K., S.H. and K.K. analysed the electrochemical data. A.M. carried out the synchrotron X-ray experiments.

Additional information

The authors declare no competing financial interests. Supplementary information accompanies this paper on www.nature.com/naturematerials. Reprints and permissions information is available online at http://www.nature.com/reprints. Correspondence and requests for materials should be addressed to R.K.